Scientific African 16 (2022) e01135

Contents lists available at ScienceDirect

Scientific African

journal homepage: www.elsevier.com/locate/sciaf

Facile synthesis of polyethylenimine-modified sugarcane bagasse adsorbent for removal of anionic dye in aqueous solution

Nurul Balqis Mohamed[a], Norzita Ngadi[a,*], Syieluing Wong[a], Noor Yahida Yahya[b], Onn Hassan[a], Ibrahim Mohammed Inuwa[c], Lawal Anako Opotu[d], Noorhalieza Ali[a]

[a] School of Chemical and Energy Engineering, Faculty of Engineering, Universiti Teknologi Malaysia, Johor 81310, Malaysia
[b] Faculty of Civil Engineering Technology, Universiti Malaysia Pahang, Lebuhraya Tun Razak, Gambang, Kuantan, Pahang 26300, Malaysia
[c] Department of Industrial Chemistry, Kaduna State University, Nigeria
[d] Department of Applied Chemistry, College of Science and Technology, Kaduna Polytechnic, Nigeria

ARTICLE INFO

Article history:
Received 28 October 2021
Revised 25 January 2022
Accepted 22 February 2022

Editor: DR B Gyampoh

Keywords:
Sugarcane bagasse
Polyethylenimine
Adsorption
Reactive black 5
Adsorbent
Agriculture waste

ABSTRACT

Many studies have reported that surface modification of various type of materials by using polyethylenimine (PEI), usually necessitate to be combined with the crosslinkers, namely glutaradehyde, sodium tripolyphosphate, etc. The sugarcane bagasse (SB) is a fibrous agricultural waste derived from sugarcane stalks residue which has rich-cellulose content that makes it amenable to surface functionalization for tailored application. Thus, it is possible for SB material to modify by using solely PEI and eliminate crosslinking step. In this study, SB was used as supporting material for modified PEI to produce polyethylenimine-modified sugarcane bagasse (PmSB) for the adsorption of Reactive Black 5 (RB5) dyes from aqueous solution. The effects of contact time (60 – 300 min), adsorbent dosage (0.05 – 0.15 g); initial dye concentration (0.01 – 0.10 g/L), pH (5 - 9) and temperature (30 – 70 °C) were varied to evaluate the performance of the PSB under different experimental conditions. The kinetics study revealed that the adsorption experimental data fitted the pseudo second order model. The equilibrium adsorption data also fitted the Langmuir model with R^2 of 0.99 and maximum monolayer capacity of 25 mg/g. The thermodynamic parameters suggest that the RB5 dye adsorption by PEI modified SB was spontaneous, exothermic and exhibited chemisorption. The adsorbent can be regenerated up to 4 cycles with the percentage dye removal greater than 80%). Therefore, the PmBS adsorbent has proven that the PEI is solely sufficient as modifying agents for SB material, even without an assistance of crosslinker reagents for removal of RB5 dye in aqueous solution.

* Corresponding author.
E-mail address: norzita@cheme.utm.my (N. Ngadi).

https://doi.org/10.1016/j.sciaf.2022.e01135

Introduction

Discharge of effluents by textile industries are frequently produce an enormous amount of synthetic dyes waste that cause severe impacts to the aquatic environment, such as instigating mutagenic and carcinogenic activities inside living cells [1,2]. There are several classifications of synthetic dyes, namely anionic dyes (direct, acid and reactive dye), cationic dyes (basic dye) or non-ionic dyes (dispersive dye), depending on the charges carried by the dye molecules when dissolved in water. The anionic dyes, which consist of azo-based chromophores, are generally used in the textile industry and constitute up to 70% of the total textile dyes. Such dyes were superior in application of textile industries due to their fastness to applied fabric, high photolytic stability, high solubility and resistance to microbial actions [3]. Reactive Black 5 (RB5) is one of the anionic dyes that often used in garment industry, due to the low cost, easy application and comparatively low toxicity. However, natural degradation and treatment of such dyes are difficult due to the high chemical stability of the dye molecules [4,5]. The reactive dyes that are mixed in water is highly resistant to fading when exposed to light and other chemical [6]. Therefore, it is important to treat the dye-containing effluent prior to discharge into the environment.

Various types of treatment techniques such as physical, chemical and advanced chemical oxidation have been developed to remove the recalcitrant dyes effectively from wastewater. However, these approaches have drawback during practical implementation because some of the treatments require high concentration of dyes for effective treatment especially in chemical precipitation techniques [6,7]. Adsorption is considered as one of the most effective method for contaminants removal among other treatment techniques (chemical precipitation, reverse osmosis, ion exchange, evaporation, filtration, oxidation/reduxtion process) because the method is versatile, results in competitive performance, no sludge generation and can be easily applied in treatment systems with high effluent flow rate [8]. The synthesis of low-cost yet effective adsorbents from various sources with tailored surface chemistries and surface properties remains a focus in the wastewater treatment. Agricultural wastes have become one of the promising materials for adsorbent preparation due to low cost, widespread availability and biodegradable [9,10]. The potential of such waste material is not fully utilized, and unplanned disposal of the waste continues to be an environmental problem [11].

Sugarcane bagasse (SB) is one of the most abundant agricultural wastes arising from the large-scale production of sugar. The global sugar production is recorded as high as 179.3 million metric tonnes (mt) in 2018/219 [11,12]. Under optimum conditions, the processing of every metric ton of sugarcane results in the production of 270 kg SB [13]. SB is a carbonaceous material containing up to 50% cellulose, 27% pentoses and 23% lignin as well as high hydroxyl and/or phenolic functional groups which exhibit metal ion-binding capacity [9]. Previous study of dyes adsorption using sugarcane bagasse without modified have reported poor adsorption capacity due to the surface functional groups are insufficient for dye removal [9,14,15]. To enhance their adsorption capacity, the SB must be chemically modified by impregnation to increase the functional group availability in the adsorbent [9].

Polyethylenimine (PEI) contains a large number of amine groups which enable reversible electrostatic binding between organic molecules and the amino groups of PEI to easily functionalize [16,17]. This is the reason PEI is often used to modify the adsorbents' surface chemistry, and many studies have demonstrated the effectiveness of PEI in enhancing the adsorbents' performance towards anionic dyes [18]. There are several type of modification methods have been used such as grafting, impregnation and others [9]. Those methods provide a high performance of the adsorbent material for pollutant adsorption (heavy metal, pharmaceuticals waste) and dyeing process. However, PEI is a water soluble material, which need for a crosslinking step to be immobilized on the cellulose to provide insoluble matrix that prevent it from leaching during adsorption process [19–21]. Commonly, the crosslinker such as glutaraldehyde [22], sodium tripolyphosphate [23] and epichlorohydrin [24] are used as the binding agent. Many study have reported about the uses of crosslinker as a binding agent in PEI modification [25,26]. However, to date, there is no report about modified of sugarcane bagasse using solely PEI (branched) as modifying agent without assistance of crosslinker which makes the facile synthesis process of the adsorbent for the removal of an anionic dyes from wastewater. The novel adsorbent not only reduces the cost of materials during synthesis, but also eliminate unnecessary toxic chemical which makes the adsorbent eco-friendly. The objectives of this study are to (1) synthesize and characterize polyethylenimine modified sugarcane bagasse (PSB) adsorbent; (2) investigate the performance of synthesized adsorbent in removal of RB5 dyes; and 3) analyze on adsorption kinetics, isotherm and thermodynamic.

Materials and methods

Materials

Sugarcane bagasse (raw SB) was obtained from the local market in Johor, Malaysia. Polyethyleneimine (PEI) (50 wt% aq solution, branched) were purchased from ACROS Organic (New Jersey, United States), potassium nitrate (KNO_3), hydrochloric acid (HCl) and sodium hydroxide (NaOH) were purchased from Sigma–Aldrich, QRec and Merck.

Synthesis of adsorbents

The raw SB were clean before cut into small pieces and dried at 70 °C for 24 h. Then, the SB was pulverized into a powder form by using a domestic grinder, followed by sieving to obtain a finely powdered with a uniform size of ~250 μm

(denoted as grounded SB (gSB)). The chemical modification of SB was performed according to the procedure described by Mohamed et al. with slight adaptations [27]. Firstly, 100 mL of PEI solution (5% w/v) was added to10 g of ground SB. Then, the mixture was stirred for 6 h at 65 °C, followed by washing of the product with deionized water to remove unattached PEI. Finally, the mixture was heated in an oven at 60 °C for 24 h. The modified adsorbent (denoted as PmSB) was kept in desiccator to minimize contact with moisture in the atmosphere.

Dye solution preparation

The RB5 stock solution was prepared by dissolving 1 g of the dye in powder form in 1000 mL of distilled water. The dye solutions with desired concentrations were then prepared by successive dilutions of the stock solution.

Preliminary study on RB5 adsorption using gSB and PmSB

The gSB and PmSB were used in the removal of RB5 from aqueous solution. The batch adsorption experiment was conducted using the conditions described by Mohamed et al. (2017), where the adsorbent dosage of 0.1 g was used in the 0.05 g/L of initial dye concentration at pH 7 for 60 to 300 min [27]. The adsorbent with a higher dye removal percentage (described in Eq. (1)) was chosen for further experiments.

$$\text{Dye removal } (\%) = \frac{(C_i - C_t)}{C_i} \times 100 \tag{1}$$

where C_i is the initial dye concentration (mg/L), C_t is the concentration at time (t) [28].

Characterization of gSB and PmSB

The gSB and PmSB were analyzed using five characterization methods. The surface functional groups were analyzed using the Fourier Transform Infrared (FTIR) Spectrometry (IRTracer-100 spectrophotometer). The measurements were conducted in the range of 450–4000 cm^{-1}. The adsorbents' surface morphology was investigated by scanning electron microscopy (SEM, JSM-6390LV, JEOL, USA). The surface area and pore size analysis were performed based on N_2 adsorption-desorption isotherm at 77 K using the Micromeritic 3 Flex Surface Characterization Analyzer, while the elemental analysis was carried out using the Perker-Elmer Elemental Analyzer Vario EL (Germany) by putting 2.0 mg of sample (solid material) into the oven at 1000 °C in which pure O_2 was injected for flash combustion process. The composition of the reaction product such as carbon, nitrogen, hydrogen and sulfur were determined. The point of zero charge analysis was performed on PmSB using a solid addition method. About 50 mL of 0.1 mol/L KNO_3 solution was added into a series of 100 mL bottles with various initial pH (2 to 10) and adjusted the pH by adding either 0.1 M of HCl or NaOH solution. After that, 0.1 g of PmSB was added into each bottle followed by shaking at 30 rpm for 24 h. The mixture was separated using a filter and the final pH of the solution was measured [29].

Adsorption experiment

Batch adsorption experiment was carried out to investigate the effects of different variables on the adsorption performance. In each experimental run, 0.1 g of adsorbent was added to 50 mL of dye solution at the desired concentration and pH in a Schott bottle (100 mL) at room temperature, and the solution was mixed thoroughly using a shaker at 180 rpm. Upon the completion of RB5 adsorption, the used adsorbent was filtered off the solution. The adsorption process was conducted by varying the following parameters: adsorbent dosage (0.05–0.15 g), initial dye concentration (0.01–0.10 g/L), pH (5–9), temperature (30–70 °C) and contact time (60–300 min). The pH of the dye solution was adjusted using 0.01 g/L of HCl (95%) and NaOH (M.Wt 40 g/mol) solutions purchased from QRec and Merck, respectively. The concentrations of the dye solution before and after adsorption were determined using the UV/Vis spectrophotometer (Shimadzu UV-1280) at 590 nm. The dye removal percentage and adsorption capacity of the adsorbent were calculated using Eqs. (1) and (2).

$$q_e = \frac{(C_i - C_t)V}{m} \tag{2}$$

where C_i is the initial dye concentration (mg/L), C_t is the concentration at time t (mg/L), V is the volume of dye solution (L), and m is the weight of dry adsorbent (g) [30].

Reusability study

The adsorbent reusability is essential for the selection of cost-effective and feasible sorbent for the pilot-scale study of an adsorption process. For the reusability study, 0.1 g of the adsorbent was added into 50 mL of RB5 solution (0.05 g/L) at pH 7 and 30 °C. After 60 min, the RB5-loaded adsorbent was filtered off the solution and dried at 70 °C for 2 h. The adsorption was repeated four times using the same adsorbent [31].

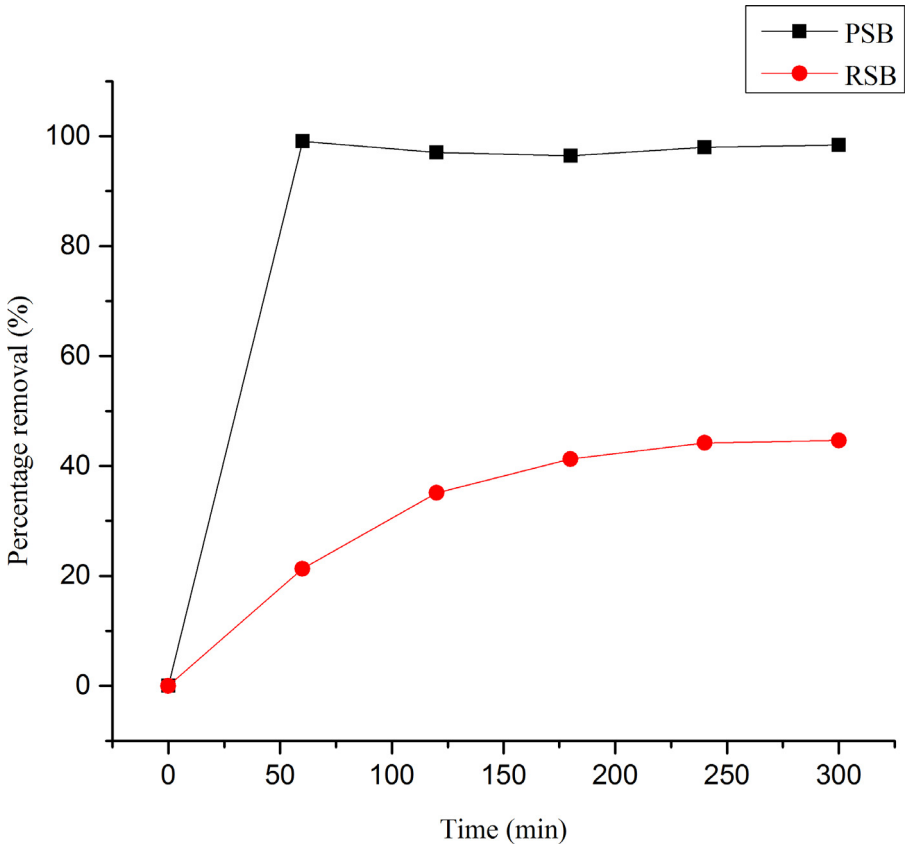

Fig. 1. The percentage removal of RB5 by gSB and PmSB.

Results and discussion

Performance of gSB and PmSB on the removal of RB5 dye

The performance of gSB and PmSB on the removal of RB5 dye was investigated to select the best adsorbents for RB5 dye. As shown in Fig. 1, when the time increased both adsorbents show the increase in percentage removal of RB5 dye. However, the percentage dye removal of gSB was lower than PmSB even with increased time. The highest percentage removal of RB5 by PmSB was nearly 100% at 60 min while the highest percentage of removal by gSB was only 45% at 300 min. The percentage removal increased at a relatively slow rate with increase in contact time due to the limited availability of active binding sited on the adsorbent surface [32,33]. The higher removal by PmSB was attributed to the presence of PEI groups on the PmSB surface which provided high surface cationic charge density [19]. PEI contain branched amine groups that bind with SO_3^{2-} groups in the RB5 molecules via electrostatic attraction forces, and hence enhances the adsorption process [34]. Therefore, PmSB was used in the subsequent adsorption experiments.

Characterization of adsorbent

The morphology and chemical structure of gSB and PmSB were studied by FTIR, BET analysis, elemental analysis and SEM analysis. FTIR spectra of gSB and PmSB are shown in Fig. 2. The gSB shows an intense band at 3402 cm^{-1}, due to O–H stretching vibration [14]. The absorption band at 2922 cm^{-1} is assigned to the C–H stretching vibration. The uronic acid ester bonds formed between the carboxylic acid group in hemicelluloses and the phenolic hydroxyl group in lignin of gSB is responsible for the peak identified at 1731 cm^{-1} [35]. The peak at 1632 cm^{-1} is attributed to the vibration of aromatic skeletal [36]. The peak at 1428 cm^{-1} is ascribed to CH_2 bending and the peak at 1374 cm^{-1} is characteristic of C–H bending which is also observed in gSB [37]. After modification, the 1731 cm^{-1} band disappeared due to degradation of ester bond [35,38]. The broad bands in the range of 3600–3200 cm^{-1} are attributed to the overlapping of the N–H band with the O–H band [17,39]. A secondary amine band was observed at 1627 cm^{-1} [39–41].

The surface area, pore size and pore volume of gSB and PmSB were determined using BET isotherm Table 1. summarizes the surface properties of gSB and PmSB. The results obtained show that the surface area of gSB was decreased after modi-

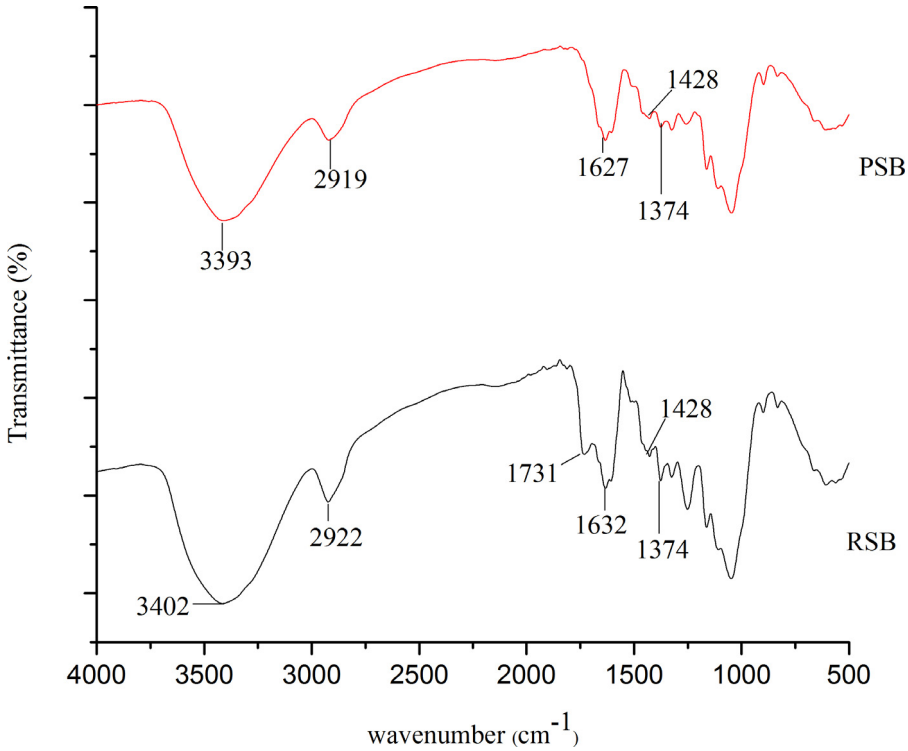

Fig. 2. FTIR spectra of gSB and PmSB.

Table 1
Textural properties of gSB and PmSB.

Adsorbent	Surface area (S_{BET}) (m^2/g)	Pore volume (cm^3/g)	Average Pore size(nm)
gSB	6.17	4.89×10^{-3}	4.51
PmSB	4.39	2.94×10^{-3}	3.88

Table 2
Elemental compositions of gSB and PmSB.

Adsorbent	N (%)	C (%)	H (%)	S (%)	C/N ratio
gSB	0.42	41.19	5.47	0.07	97.69
PmSB	2.82	41.24	5.81	0.05	14.64

fication, from 6.17 $cm^{-3}$to 4.39 cm^{-3} (PmSB) and the pore volume also decreased from 4.89×10^{-3} 2.94×10^{-3} (PSB). The previous study reported by Ahmed et al. (2017) show that when the adsorbent, sodium silicate was modified with PEI its surface area decreased from 994 m^2/g to 291 m^2/g [42]. The surface area was lower because the inner space of pores was partially filled with the PEI which blockaged the access of N_2 gas molecules into the pores and therefore results in low surface area and pore volume [42,43]. Both adsorbents were mesoporous with average pore size of 4.52 nm (gSB) and 3.88 nm (PmSB) which fall in the range of 2–5 nm (mesoporous region) [44]. The decreased average pore size after modification was due to the incorporation of amine groups into the pore structure [45,46]. This result suggests that PEI was successfully grafted on to the mesoporous SB.

The results of the elemental analysis (Table 2) confirmed the presence of PEI in the SB. There was an appreciable difference in the N concentrations of gSB and PmSB, which are 0.42% and 2.82%, respectively. The increased N content of PSB confirmed that a large amount of amine was attached to the surface of PSB [47].

In a previous study by Thakur et al. (2017), the amount of PEI grafted onto silica (MCM-41) (3.18 $mmolg^{-1}$) was calculated from the equation L_o = wt% N/(100 × 14)x1000 given the atomic mass of $N = 14$ $gmol^{-1}$. Using the equation, the amount of PEI grafted on the PmSB adsorbent was calculated to be 2.01 $gmol^{-1}$ which confirms the amount of amine group per gram of PmSB adsorbent. The surface density (d) of amine functional groups of PEI and the average intermolecular distance

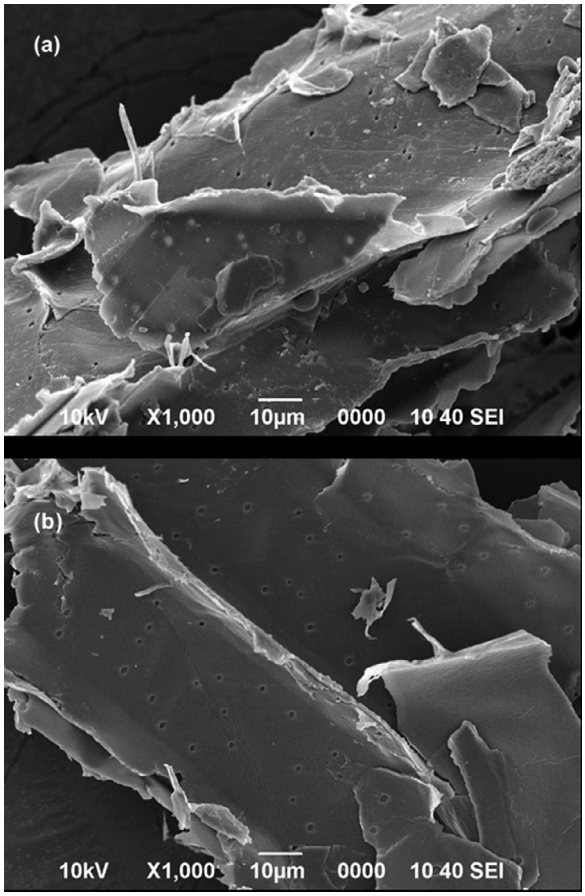

Fig. 3. Surface morphologies of (a) gSB and (b) PmSB.

(I) also can be calculated using the L_o and surface area (S_{BET}) shown in Eqs. (3) and (4) where N is Avogadro number.

$$d = N\,\frac{L_o}{S_{BET}} \tag{3}$$

$$I = \left(\frac{1}{d}\right)^{0.5} \tag{4}$$

The *d*-value for PmSB was 2.76 nm^{-2} and the distance between amine groups (I) was 0.60 nm. This result indicates that the PEI was attached efficiently on the surface of the pores in SB [45].

Additional results from SEM analysis show the difference between the gSB (Fig. 3(a) and PmSB (Fig. 3(b). SEM image of gSB (Fig. 3(a)) exhibits a less porous structure, uneven and unclear pores development which have similar characteristics with the gSB that was reported by Salihi et al. [33]. After modification with PEI (Fig. 3(b)), the PmSB surface was smoothened and porous, this is due to the impregnation of PEI which leads to blockage of the pores of SB. These results are similar to the results of the previous study on spent tea leaves modified with PEI, reported by Wong et al. [48]. The characteristics are beneficial to adsorption process, and favor dye removal capability, while indicating the presence of PEI on the SB surface [34,49].

The point of zero charge (pH_{pzc}) is about the net (external and internal) electrical neutrality of the adsorbents surface [50]. As can be seen in Fig. 4, the pH_{pzc} of PmSB was at 7.3 and it means the adsorbent is positively charged thereby favouring adsorption of the anionic dyes [51,52]. From previous study, the impregnation of PEI increased the positive charge on the adsorbent surface and leads to a higher result of pH_{pzc} [48].

The results from the FTIR, BET, SEM, elemental analysis and pH_{pzc} show the PEI was attached on the PmSB surface and that changed the properties and morphology of the gSB which means the impregnation of PEI was successful.

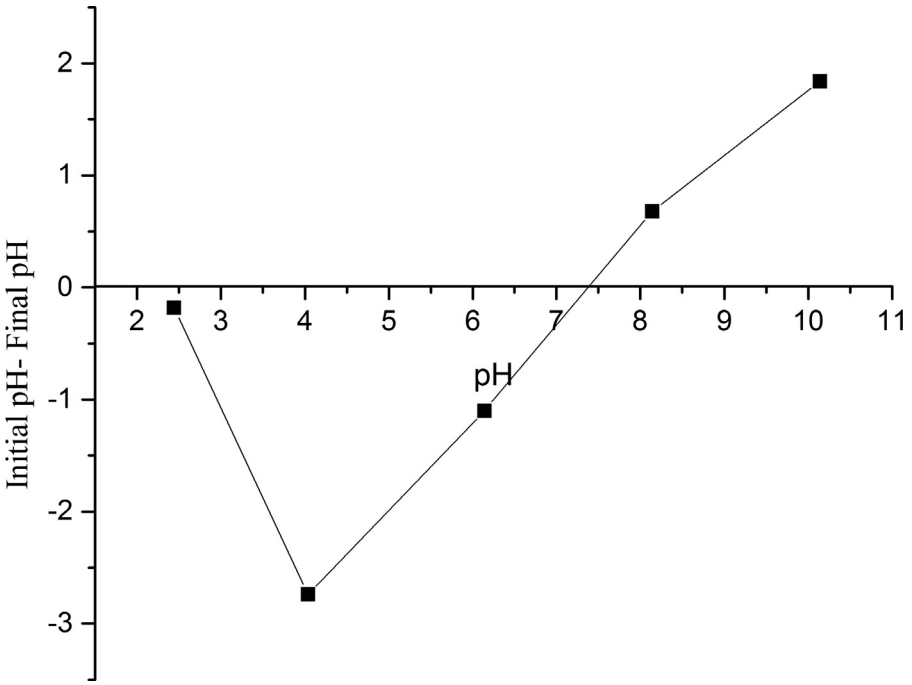

Fig. 4. Point of Zero charge of PmSB.

Effect of reaction parameters on dye adsorption

Effects of contact time

The effects of contact time on the percentage removal of RB5 and adsorption capacity of PmSB were investigated at the initial dye concentration of 0.05 g/L, pH 7, 30 °C, and adsorbent dosage of 0.1 g, with the contact time varied from 60 to 300 min Fig. 5(a) shows that the percentage removal of RB5 increased from 0% (at 0 min) to 99% (at 60 min) and began to decrease from 120 to 180 min. After that, the percentage of removal increased from 240 to 300 min. The highest RB5 removal was recorded at 60 min (99.09%) with an adsorption capacity of 24.77 mg/g. According to Fig. 5(a), 60 min is sufficient to achieve high RB5 removal, due to a large number of vacant surface sites available for adsorption at the initial stage. Following the progression of the adsorption process, the decreased number of vacant sites, together with the existence of repulsive forces between the solute molecules on the solid and the bulk phases, led to the decreased adsorption rate. A similar observation was reported by other researchers [10,53] in which adsorption increased with the contact time until a plateau was reached. The increased adsorption occurred at 240 min until 300 min due to the presence of a few surface active sites available on the surface of PmSB adsorbent [54]. This similar result was reported by Munagapati et al. [54] with the adsorption of RB5 onto banana peel powder adsorbent.

Effects of initial dye concentration

The dye percentage removal is highly dependent on the initial dye concentration, which creates the driving force to overcome mass transfer barriers between the aqueous solution and adsorbent Fig. 5(b) shows that the percentage of RB5 dye removal decreased from 99% at 0.01 g/L to 97% at 0.1 g/L of dye, due to the saturation of adsorption sites on the adsorbent surface at higher dye concentrations [55]. This occurs when at low concentration, the number of the unoccupied active sites on the adsorbent surface is high and with the increases of initial dye concentration, the required active site for the adsorption will be reduced [56]. A similar result was reported by Wong et al. [48] in the adsorption of RB5 by spent tea leaves modified with polyethylenimine adsorbent with decreased percentage removal with initial dye concentration, from 98.7 to 43.5%. This happened due to the increased proportion of dye molecules remaining in the solution. The number of available active sites on the adsorbent are fixed and are not able to remove the increasing amount of dye molecule, leading to reduction of dye percentage removal [48]. When initial dye concentration was varied from 0.01 g/L to 0.1 g/L, there was no substantial difference in adsorption capacity (24 mg/g) even though there appeared to be a slight decrease when the initial dye concentration increased. This is caused by an increase in the loading capacity of adsorbent and due to the high driving force for mass transfer at high concentration [56]. Similar results have been reported that the adsorption capacity of an adsorbent increased almost linear due to increase in binding site of the PEI on the adsorbent that increased the concentration of adsorbate removed from the aqueous solution [57]. The highest percentage removal and adsorption

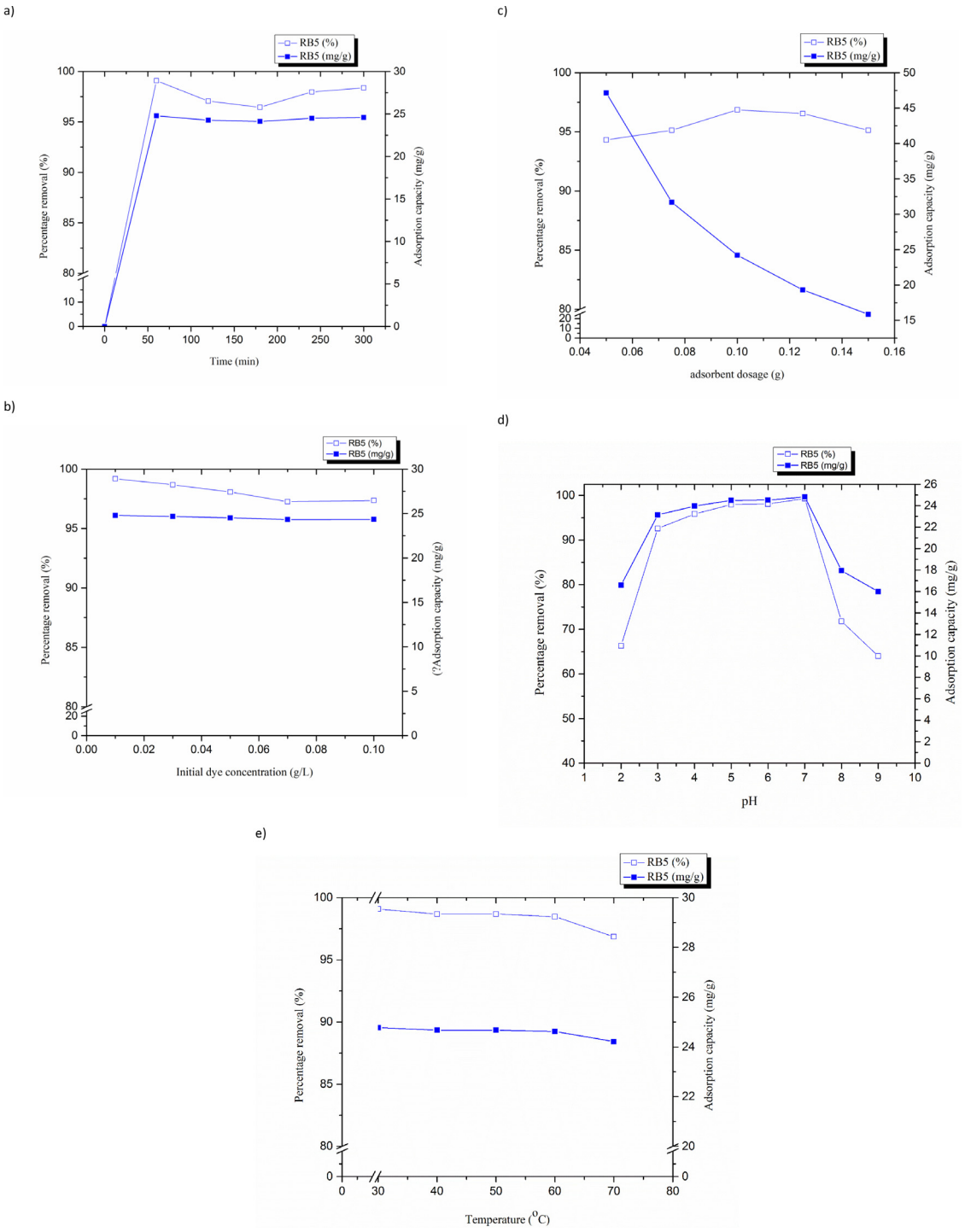

Fig. 5. Effect of a) contact time, b) initial dye concentration, c) adsorbent dosage, d) pH and e) temperature on RB5 removal by PSB.

capacity for RB5 using PmSB were observed at 0.01 g/L. The high RB5 removal observed in this study is due to increased effective interaction between the dye molecules and the adsorbent [58].

Effects of adsorbent dosage

The adsorbent dosage is another important factor in determining the capacity of the sorbent in an adsorption reaction [59]. The effects of adsorbent dosage on the percentage removal of RB5 dyes are shown in Fig. 5(c) with the initial dye

concentration of 0.05 g/L at 30 °C and pH 7 for 60 min. An increase in dye removal from 94 to 96% with adsorbent dosage was observed, which is attributed to the increased surface area and the great number of exchangeable sites available for interaction with dye molecules at higher adsorbent dosage [10]. However, the percentage of dye removal slightly decreased at adsorbent dosage of 0.1 g (97%) to 0.15 g (95%) because the available active sites were saturated and the dye molecule cannot be adsorbed [60]. Nevertheless, the percentage removal of RB5 dye was always higher than 90% within the range of adsorbent dosage used in this study, hence the effectiveness of the adsorbent and the ability of the dye to be adsorbed with minimum dosage was proven. On the other hand, the opposite trend was exhibited for adsorption capacity, which decreased with adsorbent dosage from 47.16 mg/g (0.05 g) to 15.86 mg/g (0.15 g). Such a trend occurred as the agglomeration of adsorbent at high dosage, leads to a reduced amount of active sites on the adsorbent surface [48]. The intersection of percentage removal and adsorption capacity (0.6 g/L) can introduce a good trade-off between adsorption capacity and adsorbent dosage [61].

Effects of pH

The pH determines the surface charge on the adsorbent surface and the ionization of the adsorbate molecules during the adsorption process [61]. The effects of pH (2–9) on the dye percentage removal and adsorption capacity of PmSB were studied at an initial dye concentration of 0.05 g/L, and adsorbent dosage of 0.1 g at 30 °C for 60 min Fig. 5(d) shows that the percentage dye removal increased from pH 2 (63%) to pH 7 (99%), together with an increase in adsorption capacity from 16.58 mg/g to 24.82 mg/g, due to the variation of the surface charge of the adsorbent and the ionization degree of the adsorbate It shows that pH plays an important role in adsorption. In this study, the PmSB was modified with cationic surfactant in the presence of NH^+ ions on the surface which is employed to adsorb anionic dyes [41]. The other factor that enhances the adsorption of RB5 is the repulsive energy between adsorbent [62]. In addition, the protonation of amine groups on PmSB at low pH results in a stronger electrostatic attraction between the negative charge sulphonate groups in the dye molecules and the positively charged amine groups on the adsorbent surface [61]. However, the percentage removal and adsorption capacity of RB5 decreased at higher pH values (8 to 9), because the protonation of the amine groups decreased and increased the concentration of OH^- which lead to the competition with the anionic dye and hence a weaker interaction between the dye molecules and adsorbent thereby decreasing the adsorption capacity [51,63]. The optimum pH was found to be 7 with the percentage dye removal of 99% and adsorption capacity of 24.82 mg/g. The variation in RB5 adsorption with respect to the initial solution pH can be explained with the point of zero charge (pH_{pzc}) of PSB. The results of pH_{pzc} shown in Fig. 4 indicate that the surface of PmSB is negatively charged when the pH > pH_{pzc}. For pH < pH_{pzc} the surface is positively charged and it becomes neutral at pH = pH_{pzc} [29]. This leads to a strong electrostatic attraction between the negatively charge sulfonic and ethyl sulfonic groups in RB5 molecules and the positive charge of PmSB [38].

Effect of temperature

To determine the effects of temperature on RB5 dye removal by PmSB, the experiment was carried out at 30–70 °C with an initial dye concentration of 0.05 g/L and contact time of 60 min at pH 7 with 0.1 g adsorbent Fig. 5(e) shows that the increasing temperature resulted in decreased percentage removal of dye (99% to 96%) and adsorption capacity (24.77 mg/g to 24.21 mg/g), indicating that, the adsorption process is not endothermic, but may be exothermic [64]. Increase in temperature weakens the adsorptive force between the binding sites and the dye molecules, which leads to a decrease in adsorption of RB5 [65]. On the other hand, the tendency of dye molecules to migrate from the solid phase to the aqueous phase is also affected as the temperature increases [34]. The optimum temperature was found to be 30 °C with 99% of dye removal and an adsorption capacity of 24.77 mg/g.

Kinetic study

The study on adsorption kinetics provides information on the adsorption pathway and mechanism. The influence of contact time on the amount of RB5 adsorbed by PmSB was examined to derive the adsorption kinetic parameter. The pseudo first order model (S1) describes the rate of ions uptake on ion exchange adsorbents and this rate controls the equilibrium time. On the other hand, the pseudo second order model (S2) assumes that the adsorbates are adsorbed in two active sites of the adsorbent [66].

The linear plots of log (q_e-q_t) versus t (for the pseudo first order) and t/q versus t (for the pseudo second order) are shown in Fig 6(a) and (b), respectively. The adsorption rate constants and correlation coefficients (R^2) are summarized in Table 3. A comparison was made on the fitness of the straight line of (R^2) and the q_e value Table 3. shows that the R^2 value for the pseudo second order model (0.99) was higher than R^2 value for the pseudo first order model (0.74), thus the pseudo second order model is more suitable in describing RB5 adsorption onto the PmSB. This is further supported by the observation that the predicted q_e value is close to the experimental q_e value. These observations reveal that chemisorption is more dominant in the RB5 adsorption process instead of physisorption and controlled by electrostatic attraction [67].

According to Weber and Morris models, the straight line from plotting qt versus $t^{1/2}$ indicated that the adsorption process is mainly controlled by intraparticle diffusion. However, in this study, there is multilinearity in the graph indicating that there are two or more steps involved in the adsorption process [68]. The intraparticle diffusion model (S3) is used to identify the mass transfer into the interior of the particle and the mass transfer can be described as a three-step process: (i) external mass transfer from the bulk solution to the adsorbent surface, (ii) intraparticle diffusion (iii) adsorption onto the adsorbent

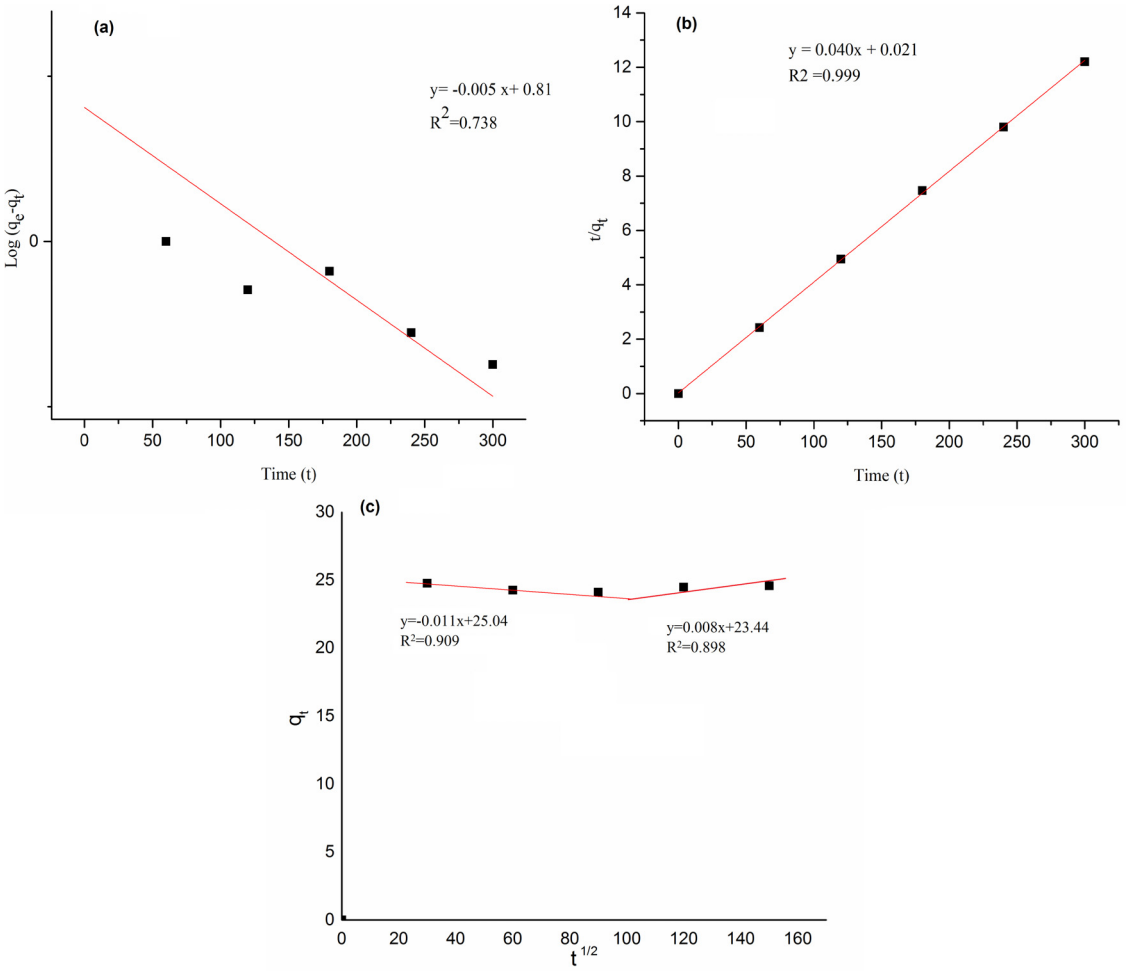

Fig. 6. Linear plots of (a) pseudo first order, (b) pseudo second order, and (c) intraparticle diffusion model for RB5 adsorption.

Table 3
Kinetic parameters of RB5 adsorption onto PmSB.

Kinetic model	Value
q_e (experiment) (mg/g)	25.00
Pseudo first orderK_1 (min^{-1})q_{eq} (mg/g)R^2	0.016.470.74
Pseudo second orderk_2 (g/(mg min)q_{eq} (mg/g)R^2	3.36×10^{-5}25.000.99
Intraparticle diffusion	
$K_{i\ 1}$ (mg g^{-1} $min^{-0.5}$)$K_{i\ 2}$ (mg g^{-1} $min^{-0.5}$)$C_1C_2R_1{}^2R_2{}^2$	0.010.00825.0423.440.910.89

surface site [69]. Two linear plots were observed in Fig 6(c), implying the occurrence of two steps in the adsorption. The first step refers to the external surface adsorption, while the second step is related to the intraparticle diffusion, where gradual adsorption of ions takes place [69,70]. The value of K_i was obtained from the slope of the linear plot of q_t versus $t^{1/2}$. The value of $K_{i\ 1}$ shows the highest *Ki* constant values which indicate that the first step is the fast step Fig. 6(c) shows that the linear plot does not pass through the origin, therefore the value of C is not equal to zero. Such observation suggests that intraparticle diffusion is not the only rate controlling step occurring in this adsorption process and probably other kinetic models may be acting in this study [68]. A similar result was also observed in the adsorption of Acid Orange 8 (AO8) and Direct Red 23 (DR23) dye onto graphene oxide [71].

Adsorption isotherm

The study on adsorption isotherm provides an insight into the interaction between the adsorbate and adsorbent in an adsorption system. The linear and nonlinear isotherm equations are included in Supplementary Materials. The Langmuir (Fig. 7(a)), Freundlich (Fig. 7(b)), and Temkin (Fig. 7(c)) models are frequently used to describe adsorption isotherms. By

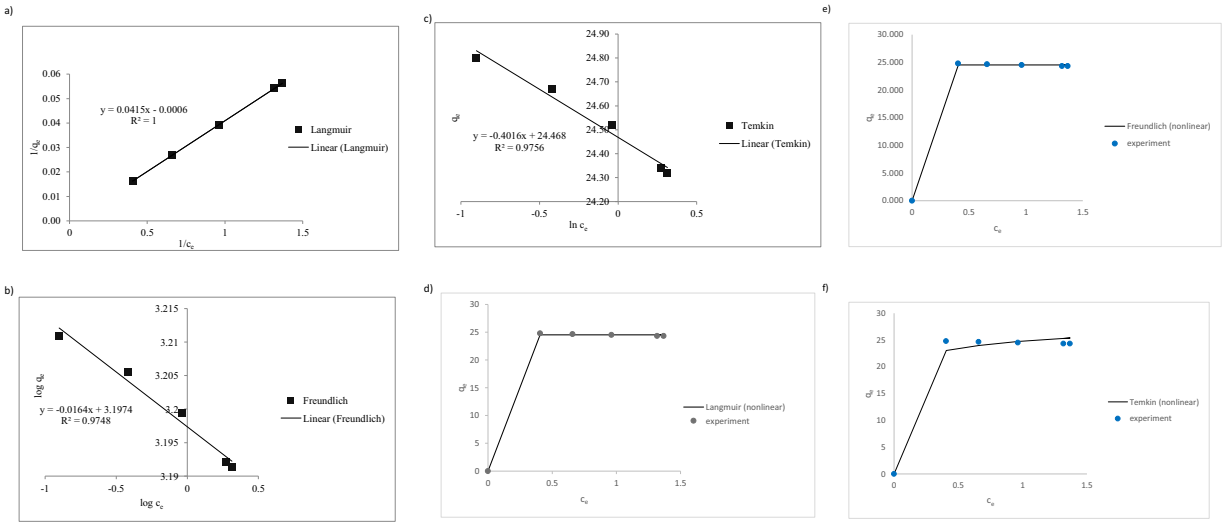

Fig. 7. Linear plots of the (a) Langmuir, (b) Freundlich and (c) Temkin model and nonlinear plot of (d) Langmuir, (e) Freundlich and (f) Temkin models for adsorption of RB5 onto PmSB.

Table 4
Models of adsorption isotherms of RB5 dye onto PmSB.

Models	Parameters	Linear	Nonlinear
Langmuir	q_{max} (mg/g)K_L (L/mg)R_LR^2	24.3910.151	24.532,185,000,0349.15 × 10^{-9}0.99
Freundlich	1/nK_F (mg/g)R^2	0.0224.460.97	024.530.99
Temkin	K_T (L/mg)b_T (kJ/mol)R^2	3.23 × 10^{27}−0.400.98	444,127.641322.390.99

fitting the q_e versus c_e plot curve, the nonlinear models of Langmuir (Fig. 7(d)), Freundlich (Fig. 7(e)), and Temkin (Fig. 7(f)) were also used to support the adsorption isotherm in this study. The essential features of the Langmuir isotherm, can be expressed in terms of separation factor (R_L) which is an important characteristic in the Langmuir model.

$$R_L = \frac{1}{1 + bC_o} \tag{12}$$

where C_o is the initial concentration of dye and b is the Langmuir constant [72]. The nature of the adsorption can be determined based on the R_L value: unfavorable (R_L>1), linear adsorption (R_L = 1), favorable (0<R_L<1) or irreversible (R_L = 0).

The Langmuir model (Table S1) indicates the occurrence of the adsorption process on the homogeneous surface of PSB with no transmigration of adsorbate in the plane of adsorbent surface. Once the active sites on PmSB are occupied with RB5 molecules, no further adsorption of RB5 can take place [73].

The maximum adsorption capacity (q_{max}) of PmSB towards RB5 dye, calculated using the linear and nonlinear Langmuir models, is 24.39 mg/g and 24.53 mg/g, respectively, as shown in Table 4. This is a favorable result due to the large quantities of primary amines contained in PEI [74]. The values of R_L for linear models (0.15) shows that the adsorption process of RB5 onto PmSB is favorable [71]. The value of R_L in nonlinear models is 9.15 × 10^{-9}, indicating that the adsorption process is favorable and that the adsorption was good [75].

The Freundlich model (Table S1) describes a multilayer adsorption process that happens on the heterogeneous surface of the adsorbent. The value of 1/n indicates the adsorption intensity of dye on the adsorbent and K_F is the adsorption capacity of the adsorbate Table 4. summarizes the values of the linear and nonlinear Freundlich constants. The value of 1/n (linear and nonlinear) is between 0 and 1, therefore the adsorption process is favorable [65,76].

The Temkin model (Table S1) is to determine the heat of adsorption and adsorbate interaction, the heat of all molecules adsorb in the layer would decrease linearly with coverage [77]. The value of b_T (Table 4) is the Temkin constant that relates to the heat of adsorption (kJ/mol) [78].

Table 4 displays the correlation coefficients (R^2) for all the models (linear and nonlinear) where the adsorption data are fitted to. Based on linear equation, the best fitting R^2 value is Langmuir model compared to the other two models, indicates that it is more suitable to describe the adsorption process. However, the R^2 value for nonlinear isotherm models shows no difference which is 0.99. When we evaluate the Langmuir model in greater detail, we can observe that the linear R2 value (1) is not significantly different from the nonlinear fitting model (0.99), but the R^2 values are still the highest when compared to other models.

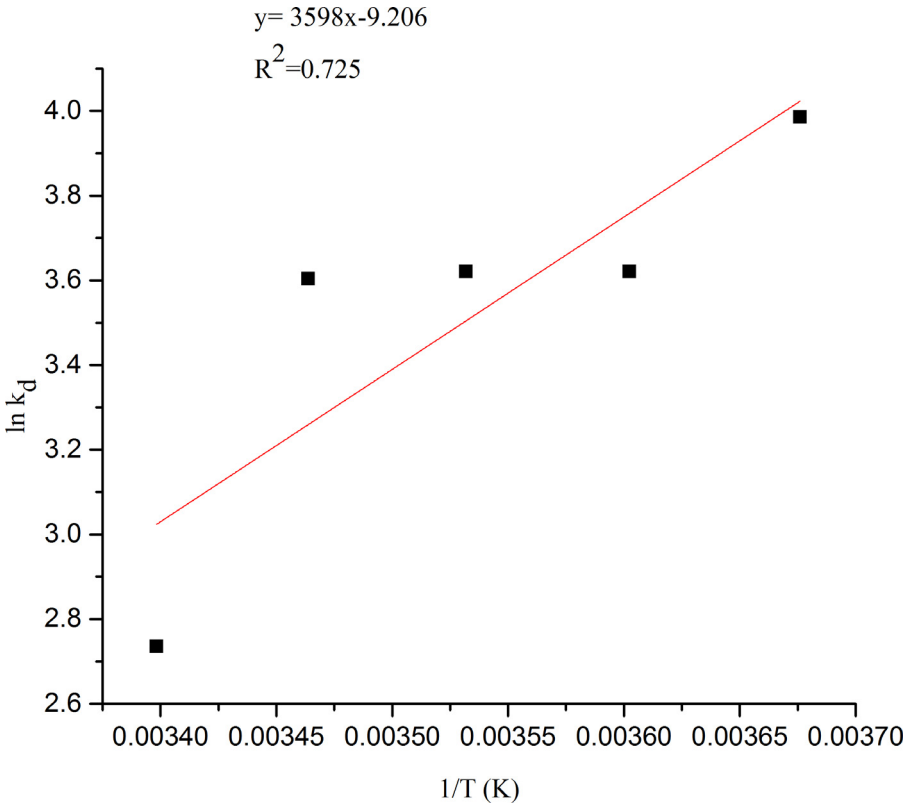

Fig. 8. Thermodynamic plot of ln k_d for RB5 adsorption on PmSB.

Table 5
Thermodynamic parameters of RB5 dye adsorption onto PmSB.

Temperature	272 K	278 K	283 K	289 K	294 K
ΔG (kJ/mol)	−9.016	−8.357	−8.542	−8.651	−6.693
ΔH (kJ/mol)	−20.822				
ΔS (J/mol K)	−76.539				

Thermodynamic study

The Thermodynamic evaluation provides important information regarding the nature and feasibility of the adsorption process. Based on Eq. (S7)), a linear plot of ln K_d versus 1/T was plotted (Fig. 8) by Van't Hoff plot to determine the values of ΔS and ΔH. The adsorption of RB5 dye on PmSB is highly temperature dependent because the distribution coefficient K_d of RB5 dye decreased linearly with increasing temperature. Increased temperature also enhances the solubility of the dyes in bulk solution more significantly than adsorbent [79]. The negative values of ΔG in Table 5 show that the adsorption of RB5 dye onto PmSB is thermodynamically feasible and spontaneous. The negative value of ΔH indicates the exothermic nature of the adsorption process. When at this condition, the dye removal by the adsorbent increases with decreased temperature [80]. This is happening due to total energy released during the bond formation between the adsorbate and adsorbent which is more than the energy released during bond breaking [81]. The value of entropy (ΔS) (−76.54 J mol^{-1} K^{-1}) suggests decreased randomness of solid-liquid interface with the structure of PmSB surface becoming more orderly after adsorption [71]. There are similar results reported by Quan et al. (2019) [82] which shows that, the adsorption of acid blue 1 onto PEI modified Cu-BTC adsorbent is exothermic, and spontaneous with entropy reduction.

Reaction mechanism of RB5 onto PmSB

The results of the adsorption of RB5 in this study show that the adsorption capacity is related to the effect of pH with the presence of electrostatic interaction between the adsorbate and adsorbent and this was proved by FTIR analysis and $pH_{pzc.}$ As shown in Fig. 2 there are two peaks at 3393 and 1627 cm^{-1} attributed to amine group after the modification with PEI solution [18]. This indicates the presence of amine on the surface of PSB after modification. From the value of pH_{pzc} and the effect of pH, it shows that adsorption of RB5 is higher at pH below 7 (Fig. 5(d)). This can be explained with the presence

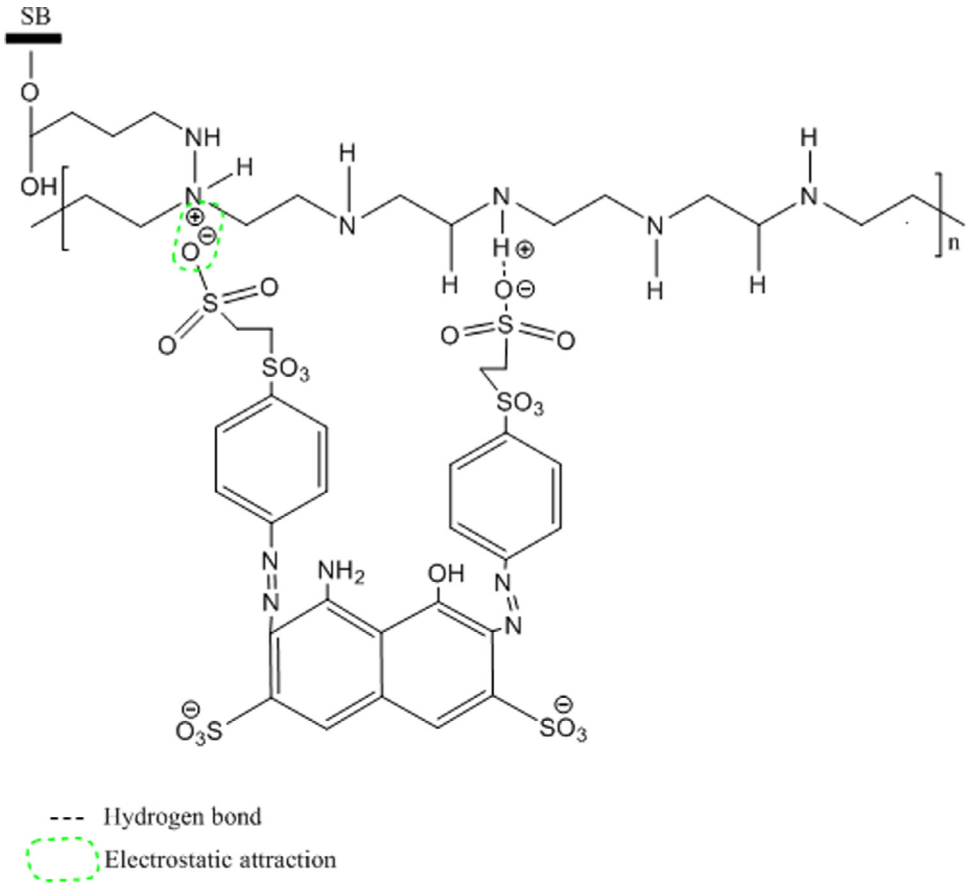

Fig. 9. Probable mechanism reaction of RB5 adsorption onto PmSB.

of anionic dye in the aqueous solution, which exists in dissociated form as anionic dye ions. In acidic, medium the amino groups will be protonated to form positively charged sites such as $-NH_3^+$, resulting in the enhanced adsorption between the dye and the adsorbent due to the significantly high electrostatic force of attraction that exists between the positively charged surface of the adsorbent (NH^+) and negative charge anionic dye (SO_3^-) [54]. Another mechanism involving hydrogen bonds may also occur in this adsorption process. PmSB contains hydroxyl or carboxyl surface groups which enables hydrogen bonding between the adsorbent and the adsorbate due to the polarization of the O–H bond. The interaction is between the H on the PmSB and Oxygen in the dye. The electrostatic attraction is between the O of SO_3^- and the protonated N on the PmSB chain According to the previous study, the adsorption of the dyes onto adsorbent modified with cationic surfactant occurs mainly through strong electrostatic interactions [48,54]. The proposed mechanism of adsorption of RB5 on PmSB is shown in Fig. 9.

Reusability study

The reusability of adsorbent is a vital factor for industrial applications. The selected adsorbent must be a cost-effective and feasible sorbent for the pilot-scale remediation system [31]. As shown in Fig. 10, the percentage of RB5 adsorption was 98% in the first run and subsequently decreased in the subsequent runs. The slight decrease in the percentage removal of RB5 dye could be due to the loss of adsorbent in the regeneration processes and irreversible binding of dyes on adsorbent [51,82]. The decrease in the percentage removal of RB5 may also be due to the loss of active site on the adsorbent [19]. Nevertheless, the removal percentage was greater than 80% up to four repeated usages. Therefore, the reusability of the PmSB adsorbent for the adsorption of anionic dye is feasible. This result highlights the potential of the PmSB adsorbent for repetitive adsorption of anionic dyes from contaminated water. The studies reported by Quan et al. [82] also highlighted similar result, in which high adsorption performance of PEI modified Cu-BTC adsorbent for acid blue 1 slowly declined after 6 cycles and the removal efficiency of the acid blue 1 remained above 80%.

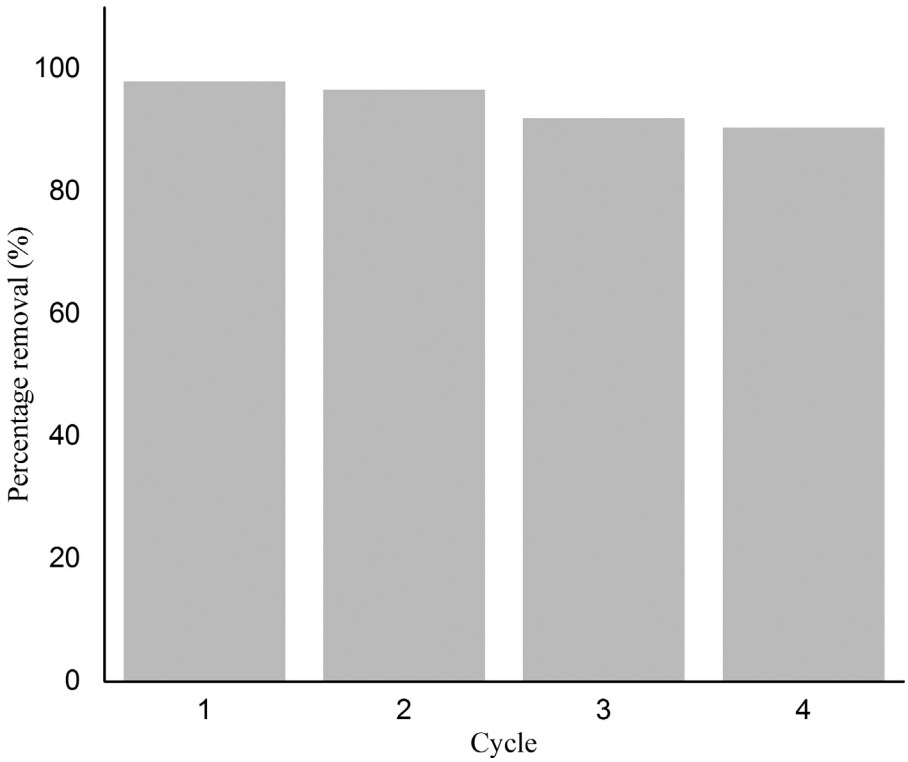

Fig. 10. Reusability of PmSB adsorbent on the RB5 adsorption.

Conclusion

This study explores the potential of SB modified with PEI as adsorbent for RB5 in aqueous solution. The PmSB adsorbent exhibited a higher adsorption performance than SB due to the presence of strong electrostatic attraction between the positively charged amine groups on the PmSB adsorbent surface and the negatively charged adsorbate. The effectiveness of PmSB as adsorbent was indicated by RB5 removal percentage greater than 90% under the studied conditions. The kinetics of RB5 dye adsorption on the PmSB adsorbent followed the pseudo second order kinetic expression; therefore, indicating that the adsorption is controlled by chemisorption. The experimental data fitted the Langmuir isotherm with the maximum adsorption capacity of 24.39 mg/g. The adsorption process was thermodynamically feasible, spontaneous and exothermic. The reusability study showed that PmSB can be reused for 4 cycles with RB5 removal percentage maintained above 80%. These results indicate that the adsorbent has a high surface area, many functional groups and easy to reuse. Therefore, the PmSB adsorbent can be a potential adsorbent with a low-cost and eco-friendly characteristic for the removal of RB5 dye from wastewater.

Declaration of Competing Interest

The authors declare that they have no known competing financial interests or personal relationships that could have appeared to influence the work reported in this paper.

Acknowledgments

The authors would like to express their sincere gratitude to the Universiti Teknologi Malaysia, for the financial support received via the Encouragement Research Grant (19J29). The lead author (Nurul Balqis Mohamed) also gratefully acknowledge the Zamalah scholarship awarded by Universiti Teknologi Malaysia.

Supplementary materials

Supplementary material associated with this article can be found, in the online version, at doi:10.1016/j.sciaf.2022.e01135.

References

[1] T. Ahmad, M. Danish, Prospects of banana waste utilization in wastewater treatment: a review, J. Environ. Manag. 206 (2018) 330–348, doi:10.1016/j.jenvman.2017.10.061.

[2] A.A. Peláez-Cid, V. Romero-Hernández, A.M. Herrera-González, A. Bautista-Hernández, O. Coreño-Alonso, Synthesis of activated carbons from black sapote seeds, characterization and application in the elimination of heavy metals and textile dyes, Chin. J. Chem. Eng. 28 (2020) 613–623, doi:10.1016/j.cjche.2019.04.021.

[3] R. Hickman, E. Walker, S. Chowdhury, Journal of Water Process Engineering TiO_2 -PDMS composite sponge for adsorption and solar mediated photodegradation of dye pollutants, J. Water Process Eng. 24 (2018) 74–82, doi:10.1016/j.jwpe.2018.05.015.

[4] M. Chang, Y. hsin Shih, Synthesis and application of magnetic iron oxide nanoparticles on the removal of reactive black 5: reaction mechanism, temperature and pH effects, J. Environ. Manag. 224 (2018) 235–242, doi:10.1016/j.jenvman.2018.07.021.

[5] F. Iranpour, H. Pourzamani, N. Mengelizadeh, P. Bahrami, H. Mohammadi, Application of response surface methodology for optimization of reactive black 5 removal by three dimensional electro-Fenton process, J. Environ. Chem. Eng. 6 (2018) 3418–3435, doi:10.1016/j.jece.2018.05.023.

[6] S. Mishra, A. Maiti, The efficacy of bacterial species to decolourise reactive azo, anthroquinone and triphenylmethane dyes from wastewater: a review, Environ. Sci. Pollut. Res. 25 (2018) 8286–8314, doi:10.1007/s11356-018-1273-2.

[7] J.K. Bediako, S. Lin, A.K. Sarkar, Y. Zhao, J.W. Choi, M.H. Song, C.W. Cho, Y.S. Yun, Evaluation of orange peel-derived activated carbons for treatment of dye-contaminated wastewater tailings, Environ. Sci. Pollut. Res. (2019), doi:10.1007/s11356-019-07031-8.

[8] S.J. Segovia-Sandoval, R. Ocampo-Pérez, M.S. Berber-Mendoza, R. Leyva-Ramos, A. Jacobo-Azuara, N.A. Medellín-Castillo, Walnut shell treated with citric acid and its application as biosorbent in the removal of Zn(II), J. Water Process Eng. 25 (2018) 45–53, doi:10.1016/j.jwpe.2018.06.007.

[9] W. Jiang, Y. Xing, L. Zhang, X. Guo, Y. Lu, M. Yang, J. Wang, G. Wei, Polyethylenimine-modified sugarcane bagasse cellulose as an effective adsorbent for removing Cu(II) from aqueous solution, J. Appl. Polym. Sci. (2020) 1–14, doi:10.1002/app.49830.

[10] A.E.A.A. Said, A.A.M. Aly, M.N. Goda, M. Abd El-Aal, M. Abdelazim, Modified sugarcane bagasse with tartaric acid for removal of diazonium blue from aqueous solutions, J. Polym. Environ. 26 (2018) 2424–2433, doi:10.1007/s10924-017-1136-9.

[11] S.A. Mangi, N. Jamaluddin, M.H. Wan Ibrahim, A.H. Abdullah, Utilization of sugarcane bagasse ash in concrete as partial replacement of cement utilization of sugarcane bagasse ash in concrete as partial replacement of cement, Conf. Ser. Mater. Sci. Eng. (2017), doi:10.1088/1757-899X/271/1/012001.

[12] Food and Agriculture Organization of the United Nations (FAO), Market Assessments: Sugar, Food Outlook - Biannu. Rep. Glob. Food Mark. (2019) 1–6. https://www.fao.org/3/ca4526en/ca4526en.pdf

[13] N. Sahiron, N. Rahmat, F. Hamzah, Characterization of sodium silicate derived from sugarcane bagasse ash, Malays. J. Anal. Sci. 21 (2017) 512–517, doi:10.17576/mjas-2017-2102-26.

[14] M. Ge, M. Du, L. Zheng, B. Wang, X. Zhou, Z. Jia, G. Hu, S.M. Jahangir Alam, A maleic anhydride grafted sugarcane bagasse adsorbent and its performance on the removal of methylene blue from related wastewater, Mater. Chem. Phys. 192 (2017) 147–155, doi:10.1016/j.matchemphys.2017.01.063.

[15] J.Y.W. Xiong, J. Zhu, J.C.R. Chi, Removal of Congo red from aqueous solution by adsorption onto different amine compounds modified sugarcane bagasse, Clean Technol. Environ. Policy 19 (2017) 517–525, doi:10.1007/s10098-016-1243-7.

[16] A.N. Solodov, J.R. Shayimova, E.A. Burilova, R.R. Amirov, Polyethyleneimine-modified iron oxide nanoparticles : their synthesis and state in water and in solutions of ligands, Colloid Polym. Sci. (2018) 1983–1993, doi:10.1007/s00396-018-4425-5.

[17] Z. He, H. Song, Y. Cui, W. Zhu, K. Du, S. Yao, Porous spherical cellulose carrier modified with polyethyleneimine and its adsorption for Cr(III) and Fe(III) from aqueous solutions, Chin. J. Chem. Eng. 22 (2014) 984–990, doi:10.1016/j.cjche.2014.07.001.

[18] M.H. Kim, C.H. Hwang, S. Bin Kang, S. Kim, S.W. Park, Y.S. Yun, S.W. Won, Removal of hydrolyzed reactive black 5 from aqueous solution using a polyethylenimine–polyvinyl chloride composite fiber, Chem. Eng. J. 280 (2015) 18–25, doi:10.1016/j.cej.2015.05.069.

[19] S. Tangtubtim, S. Saikrasun, Applied surface science adsorption behavior of polyethyleneimine-carbamate linked pineapple leaf fi ber for Cr (VI) removal, Appl. Surf. Sci. 467–468 (2019) 596–607, doi:10.1016/j.apsusc.2018.10.204.

[20] H. Zeng, L. Wang, D. Zhang, P. Yan, J. Nie, V.K. Sharma, Highly e ffi cient and selective removal of mercury ions using hyperbranched polyethylenimine functionalized carboxymethyl chitosan composite adsorbent, Chem. Eng. J. 358 (2019) 253–263, doi:10.1016/j.cej.2018.10.001.

[21] N.H. Yusof, K.Y. Foo, B.H. Hameed, M.H. Hussin, H.K. Lee, S. Sabar, International journal of biological macromolecules one-step synthesis of chitosan-polyethyleneimine with calcium chloride as effective adsorbent for acid red 88 removal, Int. J. Biol. Macromol. 157 (2020) 648–658, doi:10.1016/j.ijbiomac.2019.11.218.

[22] B. Chen, Y. Liu, S. Chen, X. Zhao, X. Meng, X. Pan, Magnetically recoverable cross-linked polyethylenimine as a novel adsorbent for removal of anionic dyes with different structures from aqueous solution, J. Taiwan Inst. Chem. Eng. 67 (2016) 191–201, doi:10.1016/j.jtice.2016.07.014.

[23] A. Mokhtar, S. Abdelkrim, A. Djelad, A. Sardi, B. Boukoussa, M. Sassi, A. Bengueddach, Adsorption behavior of cationic and anionic dyes on magadiite-chitosan composite beads, Carbohydr. Polym. 229 (2020) 115399, doi:10.1016/j.carbpol.2019.115399.

[24] N.A. Negm, H.H.H. Hefni, A.A.A. Abd-elaal, E.A. Badr, M.T.H. Abou, International journal of biological macromolecules advancement on modi fi cation of chitosan biopolymer and its potential applications, Int. J. Biol. Macromol. 152 (2020) 681–702, doi:10.1016/j.ijbiomac.2020.02.196.

[25] J. Tang, L. Xiang, J. Fan, Z. Cui, H. Wu, Synthesis of polyethylenimine-functionalized magnetic materials and a critical evaluation of the removal of copper in sediments, Environ. Earth Sci. 77 (2018) 1–8, doi:10.1007/s12665-018-7647-4.

[26] Suhas, V.K. Gupta, P.J.M. Carrott, R. Singh, M. Chaudhary, S. Kushwaha, Cellulose: a review as natural, modified and activated carbon adsorbent, Bioresour. Technol. 216 (2016) 1066–1076, doi:10.1016/j.biortech.2016.05.106.

[27] N.B. Mohamed, N. Ngadi, N.S. Lani, R. Ab, Polyethylenimine modified sugarcane bagasse adsorbent for methyl orange dye removal, Chem. Eng. Trans. 56 (2017) 103–108, doi:10.3303/CET1756018.

[28] M. Dehvari, M. Ghaneian, A. Ebrahimi, B. Jamshidi, M. Mootab, Removal of reactive blue 19 dyes from textile wastewater by pomegranate seed powder: isotherm and kinetic studies, Int. J. Environ. Health Eng. 5 (2016) 5, doi:10.4103/2277-9183.179204.

[29] R.A.K. Rao, U. Khan, Adsorption of Ni(II) on alkali treated pineapple residue (Ananas comosus L.): batch and column studies, Groundw. Sustain. Dev. 5 (2017) 244–252, doi:10.1016/j.gsd.2017.08.002.

[30] Z. Zhu, P. Wu, G. Liu, X. He, B. Qi, G. Zeng, W. Wang, Y. Sun, F. Cui, Ultrahigh adsorption capacity of anionic dyes with sharp selectivity through the cationic charged hybrid nanofibrous membranes, Chem. Eng. J. 313 (2017) 957–966, doi:10.1016/j.cej.2016.10.145.

[31] T.A. Saleh, M.Tuzen Naeemullah, A. Sarı, Polyethylenimine modified activated carbon as novel magnetic adsorbent for the removal of uranium from aqueous solution, Chem. Eng. Res. Des. 117 (2017) 218–227, doi:10.1016/j.cherd.2016.10.030.

[32] C. Liu, R.N. Jin, X. kun Ouyang, Y.G. Wang, Adsorption behavior of carboxylated cellulose nanocrystal-polyethyleneimine composite for removal of Cr(VI) ions, Appl. Surf. Sci. 408 (2017) 77–87, doi:10.1016/j.apsusc.2017.02.265.

[33] I.U. Salihi, S.R. Kutty, M. Isa, E. Olisa, N. Aminu, Adsorption of copper using modified and unmodified sugarcane bagasse, Int. J. Appl. Eng. Res. 10 (2015) 40434–40438 https://www.scopus.com/inward/record.uri?eid=2-s2.0-84945897011&partnerID=40&md5=c5050352f683a054e2e8e260a3dddbd5.

[34] S. Hena, S. Atikah, H. Ahmad, Removal of phosphate ion from water using chemically modified biomass of sugarcane bagasse, Int. J. Eng. Sci. 4 (2015) 51–62.

[35] S. Luo, S. Chen, S. Chen, L. Zhuang, N. Ma, T. Xu, Q. Li, X. Hou, Preparation and characterization of amine-functionalized sugarcane bagasse for CO_2 capture, J. Environ. Manag. 168 (2016) 142–148, doi:10.1016/j.jenvman.2015.09.033.

[36] F. Wang, Y. Pan, P. Cai, T. Guo, H. Xiao, Single and binary adsorption of heavy metal ions from aqueous solutions using sugarcane cellulose-based adsorbent, Bioresour. Technol. 241 (2017) 482–490, doi:10.1016/j.biortech.2017.05.162.

[37] Y.H. Feng, T.Y. Cheng, W.G. Yang, P.T. Ma, H.Z. He, X.C. Yin, X.X. Yu, Characteristics and environmentally friendly extraction of cellulose nanofibrils from sugarcane bagasse, Ind. Crops Prod. 111 (2018) 285–291, doi:10.1016/j.indcrop.2017.10.041.

[38] Z. Jiang, D. Hu, Molecular mechanism of anionic dyes adsorption on cationized rice husk cellulose from agricultural wastes, J. Mol. Liq. 276 (2019) 105–114, doi:10.1016/j.molliq.2018.11.153.
[39] H. Ah, H. Neul, S. Wook, A reusable adsorbent polyethylenimine /polyvinyl chloride crosslinked fi ber for Pd (II) recovery from acidic solutions, J. Environ. Manag. 204 (2017) 200–206, doi:10.1016/j.jenvman.2017.08.047.
[40] G.M. Kim, Z. Wang, S. Bin Kang, S.W. Won, Polyethylenimine-crosslinked chitin flake as a biosorbent for removal of acid blue 25, Korean J. Chem. Eng. 36 (2019) 1455–1465, doi:10.1007/s11814-019-0347-2.
[41] H.W. Kwak, K.H. Lee, Polyethylenimine-functionalized silk sericin beads for high-performance remediation of hexavalent chromium from aqueous solution, Chemosphere 207 (2018) 507–516, doi:10.1016/j.chemosphere.2018.04.158.
[42] S. Ahmed, A. Ramli, S. Yusup, Development of polyethylenimine-functionalized mesoporous Si-MCM-41 for CO 2 adsorption, Fuel Process. Technol. 167 (2017) 622–630, doi:10.1016/j.fuproc.2017.07.036.
[43] Y. He, Q. Liu, J. Hu, C. Zhao, C. Peng, Q. Yang, H. Wang, H. Liu, Efficient removal of Pb(II) by amine functionalized porous organic polymer through post-synthetic modification, Sep. Purif. Technol. 180 (2017) 142–148, doi:10.1016/j.seppur.2017.01.026.
[44] D. Jiang, F. Wang, B. Lan, D. Wang, K. Liang, T. Li, D. Zhao, J. Chen, J. Lin, W. Chan, Y. Li, Efficient treatment of anthraquinone dye wastewater by adsorption using sunflower torus-like magnesium hydroxide microspheres, Korean J. Chem. Eng. 37 (2020) 434–447, doi:10.1007/s11814-019-0455-z.
[45] A.K. Thakur, G.M. Nisola, L.A. Limjuco, K.J. Parohinog, R.E.C. Torrejos, V.K. Shahi, W.J. Chung, Polyethylenimine-modified mesoporous silica adsorbent for simultaneous removal of Cd(II) and Ni(II) from aqueous solution, J. Ind. Eng. Chem. 49 (2017) 133–144, doi:10.1016/j.jiec.2017.01.019.
[46] M. Ojeda, M. Mazaj, S. Garcia, J. Xuan, M.M. Maroto-Valer, N.Z. Logar, Novel amine-impregnated mesostructured silica materials for CO_2capture, Energy Procedia 114 (2017) 2252–2258, doi:10.1016/j.egypro.2017.03.1362.
[47] B. Li, Q. Wang, J.Z. Guo, W.W. Huan, L. Liu, Sorption of methyl orange from aqueous solution by protonated amine modified hydrochar, Bioresour. Technol. 268 (2018) 454–459, doi:10.1016/j.biortech.2018.08.023.
[48] S. Wong, H.H. Tumari, N. Ngadi, N.B. Mohamed, O. Hassan, R. Mat, N. Aishah, S. Amin, Adsorption of anionic dyes on spent tea leaves modi fi ed with polyethyleneimine (PEI-STL), J. Clean. Prod. 206 (2019) 394–406, doi:10.1016/j.jclepro.2018.09.201.
[49] L.S. Silva, F.J.L. Ferreira, M.S. Silva, A.M.G.L. Citó, A.B. Meneguin, R.M. Sábio, H.S. Barud, R.D.S. Bezerra, J.A. Osajima, E.C. Silva Filho, Potential of amino-functionalized cellulose as an alternative sorbent intended to remove anionic dyes from aqueous solutions, Int. J. Biol. Macromol. 116 (2018) 1282–1295, doi:10.1016/j.ijbiomac.2018.05.034.
[50] M. Thi, H. Chao, T. Van Trinh, T. Thi, C. Lin, Removal of ammonium from groundwater using NaOH-treated activated carbon derived from corncob wastes : batch and column experiments, J. Clean. Prod. 180 (2018) 560–570, doi:10.1016/j.jclepro.2018.01.104.
[51] Y. Long, L. Xiao, Q. Cao, Co-polymerization of catechol and polyethylenimine on magnetic nanoparticles for efficient selective removal of anionic dyes from water, Powder Technol. 310 (2017) 24–34, doi:10.1016/j.powtec.2017.01.013.
[52] R. Lafi, A. Hafiane, Removal of methyl orange (MO) from aqueous solution using cationic surfactants modified coffee waste (MCWs), J. Taiwan Inst. Chem. Eng. 000 (2015) 1–10, doi:10.1016/j.jtice.2015.06.035.
[53] L. Divband Hafshejani, A. Hooshmand, A.A. Naseri, A.S. Mohammadi, F. Abbasi, A. Bhatnagar, Removal of nitrate from aqueous solution by modified sugarcane bagasse biochar, Ecol. Eng. 95 (2016) 101–111, doi:10.1016/j.ecoleng.2016.06.035.
[54] V.S. Munagapati, V. Yarramuthi, Y. Kim, K.M. Lee, D.S. Kim, Removal of anionic dyes (reactive black 5 and congo red) from aqueous solutions using banana peel powder as an adsorbent, Ecotoxicol. Environ. Saf. 148 (2018) 601–607, doi:10.1016/j.ecoenv.2017.10.075.
[55] G.B. Oguntimein, Biosorption of dye from textile wastewater effluent onto alkali treated dried sunflower seed hull and design of a batch adsorber, J. Environ. Chem. Eng. 3 (2015) 2647–2661, doi:10.1016/j.jece.2015.09.028.
[56] X. Xu, B. Bai, H. Wang, Y. Suo, Enhanced adsorptive removal of Safranine T from aqueous solutions by waste sea buckthorn branch powder modi fi ed with dopamine : kinetics, equilibrium, and thermodynamics, J. Phys. Chem. Solids 87 (2015) 23–31, doi:10.1016/j.jpcs.2015.07.022.
[57] Y. Lu, L. Fan, L.Y. Yang, F. Huang, X. kun Ouyang, PEI-modified core-shell/bead-like amino silica enhanced poly (vinyl alcohol)/chitosan for diclofenac sodium efficient adsorption, Carbohydr. Polym. 229 (2020) 115459, doi:10.1016/j.carbpol.2019.115459.
[58] D. Robati, B. Mirza, M. Rajabi, O. Moradi, I. Tyagi, S. Agarwal, V.K. Gupta, Removal of hazardous dyes-BR 12 and methyl orange using graphene oxide as an adsorbent from aqueous phase, Chem. Eng. J. 284 (2016) 687–697, doi:10.1016/j.cej.2015.08.131.
[59] H. Singh, G. Chauhan, A.K. Jain, S.K. Sharma, Adsorptive potential of agricultural wastes for removal of dyes from aqueous solutions, J. Environ. Chem. Eng. 5 (2017) 122–135, doi:10.1016/j.jece.2016.11.030.
[60] R. Huang, Q. Liu, J. Huo, B. Yang, Adsorption of methyl orange onto protonated cross-linked chitosan, Arab. J. Chem. 10 (2017) 24–32, doi:10.1016/j.arabjc.2013.05.017.
[61] W. Wang, G. Huang, C. An, S. Zhao, X. Chen, P. Zhang, Adsorption of anionic azo dyes from aqueous solution on cationic gemini surfactant-modified flax shives: synchrotron infrared, optimization and modeling studies, J. Clean. Prod. 172 (2018) 1986–1997, doi:10.1016/j.jclepro.2017.11.227.
[62] X. Sun, H. Ou, C. Miao, L. Chen, Removal of sudan dyes from aqueous solution by magnetic carbon nanotubes: equilibrium, kinetic and thermodynamic studies, J. Ind. Eng. Chem. 22 (2015) 373–377, doi:10.1016/j.jiec.2014.07.034.
[63] S. Tangtubtim, S. Saikrasun, Adsorption behavior of polyethyleneimine-carbamate linked pineapple leaf fiber for Cr(VI) removal, Appl. Surf. Sci. 467–468 (2019) 596–607, doi:10.1016/j.apsusc.2018.10.204.
[64] H. Tahir, M. Sultan, N. Akhtar, U. Hameed, T. Abid, Application of natural and modified sugar cane bagasse for the removal of dye from aqueous solution, J. Saudi Chem. Soc. 20 (2016) S115–S121, doi:10.1016/j.jscs.2012.09.007.
[65] K.S. Thangamani, N. Muthulakshmi Andal, E. Ranjith Kumar, M. Saravanabhavan, Utilization of magnetic nano cobalt ferrite doped capra aegagrus hircus dung activated carbon composite for the adsorption of anionic dyes, J. Environ. Chem. Eng. 5 (2017) 2820–2829, doi:10.1016/j.jece.2017.05.030.
[66] A. Macías-García, M. Gómez Corzo, M. Alfaro Domínguez, M. Alexandre Franco, J. Martínez Naharro, Study of the adsorption and electroadsorption process of Cu (II) ions within thermally and chemically modified activated carbon, J. Hazard. Mater. 328 (2017) 46–55, doi:10.1016/j.jhazmat.2016.11.036.
[67] W.X. Zhang, L. Lai, P. Mei, Y. Li, Y.H. Li, Y. Liu, Enhanced removal efficiency of acid red 18 from aqueous solution using wheat bran modified by multiple quaternary ammonium salts, Chem. Phys. Lett. 710 (2018) 193–201, doi:10.1016/j.cplett.2018.09.009.
[68] K.B. Fontana, E.S. Chaves, J.D.S. Sanchez, E.R.L.R. Watanabe, J.M.T.A. Pietrobelli, G.G. Lenzi, Textile dye removal from aqueous solutions by malt bagasse: isotherm, kinetic and thermodynamic studies, Ecotoxicol. Environ. Saf. 124 (2016) 329–336, doi:10.1016/j.ecoenv.2015.11.012.
[69] N. Maaloul, P. Oulego, M. Rendueles, A. Ghorbal, M. Díaz, Novel biosorbents from almond shells : characterization and adsorption properties modeling for Cu (II) ions from aqueous solutions, J. Environ. Chem. Eng. 5 (2017) 2944–2954, doi:10.1016/j.jece.2017.05.037.
[70] J.X. Yang, G.B. Hong, Adsorption behavior of modified Glossogyne tenuifolia leaves as a potential biosorbent for the removal of dyes, J. Mol. Liq. 252 (2018) 289–295, doi:10.1016/j.molliq.2017.12.142.
[71] W. Konicki, M. Aleksandrzak, D. Moszyński, E. Mijowska, Adsorption of anionic azo-dyes from aqueous solutions onto graphene oxide: equilibrium, kinetic and thermodynamic studies, J. Colloid Interface Sci. 496 (2017) 188–200, doi:10.1016/j.jcis.2017.02.031.
[72] H. Chaudhuri, S. Dash, S. Ghorai, S. Pal, A. Sarkar, SBA-16: application for the removal of neutral, cationic, and anionic dyes from aqueous medium, J. Environ. Chem. Eng. 4 (2016) 157–166, doi:10.1016/j.jece.2015.11.020.
[73] N.A. Dahlan, S.L. Ng, J. Pushpamalar, Adsorption of methylene blue onto powdered activated carbon immobilized in a carboxymethyl sago pulp hydrogel, J. Appl. Polym. Sci. 134 (2017) 1–11, doi:10.1002/app.44271.
[74] X. Jin, Z. Xiang, Q. Liu, Y. Chen, F. Lu, Polyethyleneimine-bacterial cellulose bioadsorbent for effective removal of copper and lead ions from aqueous solution, Bioresour. Technol. 244 (2017) 844–849, doi:10.1016/j.biortech.2017.08.072.
[75] İ. Şentürk, M.R. Yıldız, Highly efficient removal from aqueous solution by adsorption of Maxilon red GRL dye using activated pine sawdust, Korean J. Chem. Eng. 37 (2020) 985–999, doi:10.1007/s11814-020-0526-1.

[76] C.K. Aslani, O. Amik, Active carbon/pan composite adsorbent for uranium removal: modeling adsorption isotherm data, thermodynamic and kinetic studies, Appl. Radiat. Isot. 168 (2021) 109474, doi:10.1016/j.apradiso.2020.109474.
[77] S.C. Cheu, H. Kong, T. Song, N. Saman, RSC advances high removal performance of dissolved oil from aqueous solution by sorption using fatty acid esteri fi ed pineapple leaves as novel sorbents, R. Soc. Chem. (2016) 13710–13722, doi:10.1039/c5ra22929d.
[78] S.M.A. El-Gamal, M.S. Amin, M.A. Ahmed, Removal of methyl orange and bromophenol blue dyes from aqueous solution using Sorel's cement nanoparticles, J. Environ. Chem. Eng. 3 (2015) 1702–1712, doi:10.1016/j.jece.2015.06.022.
[79] S. Chan, Y. Ping, A. Halim, S. Ong, Journal of the Taiwan institute of chemical engineers equilibrium, kinetic and thermodynamic studies of a new potential biosorbent for the removal of basic blue 3 and congo red dyes : pineapple (Ananas comosus) plant stem, J. Taiwan Inst. Chem. Eng. 61 (2016) 306–315, doi:10.1016/j.jtice.2016.01.010.
[80] M. Junqueira, P. Brito, C.M. Veloso, L.S. Santos, R. Cristina, F. Bonomo, C. Ilhéu, Adsorption of the textile dye Dianix ® royal blue CC onto carbons obtained from yellow mombin fruit stones and activated with KOH and H 3 PO 4 : kinetics, adsorption equilibrium and thermodynamic studies, Powder Technol. 339 (2018) 334–343, doi:10.1016/j.powtec.2018.08.017.
[81] F. Arshad, M. Selvaraj, J. Zain, F. Banat, M. Abu, Separation and Puri fi cation technology polyethylenimine modi fi ed graphene oxide hydrogel composite as an e ffi cient adsorbent for heavy metal ions, Sep. Purif. Technol. 209 (2019) 870–880, doi:10.1016/j.seppur.2018.06.035.
[82] X. Quan, Z. Sun, H. Meng, Y. Han, J. Wu, J. Xu, Y. Xu, X. Zhang, Polyethyleneimine (PEI) incorporated Cu-BTC composites: extended applications in ultra-high efficient removal of congo red, J. Solid State Chem. 270 (2019) 231–241, doi:10.1016/j.jssc.2018.11.021.